NMC NOTES

The New NMC Mesoscale Eta Model: Description and Forecast Examples

THOMAS L. BLACK

Development Division, National Meteorological Center, NWS/NOAA, Washington, D.C.

25 October 1993 and 1 February 1994

ABSTRACT

In mid-1994 a new version of the Eta Model will begin producing operational forecast guidance down to mesoscale ranges. This version will have a horizontal resolution of approximately 30 km and about 50 layers in the vertical. A summary of the primary aspects of the model is presented that includes a description of the eta coordinate and of the dynamical and physical components. Advantages of the mesoscale model are indicated in precipitation skill scores for November 1993. Specific examples are discussed that describe the mesoscale model's ability to capture small-scale circulations under fundamentally different circumstances: (i) the propagation of a strong cold front where the forcing was primarily internal and not orographic; and (ii) a rainfall event where the forcing arose from the interaction of topography with the synoptic-scale flow.

1. Introduction

As computer technology continues to improve, and the quantity and quality of atmospheric observations increase, the generation of mesoscale forecast guidance over the United States in an operational mode is becoming increasingly feasible. Providing such guidance is the goal of the National Meteorological Center's (NMC's) effort in developing the step-mountain eta coordinate model generally known as the Eta model. Considerable development has taken place using a synoptic-scale version with 80-km horizontal resolution to improve many of the specifications and parameterizations of the model. This version replaced the Limited-Area Fine Mesh Model (LFM) in June 1993 as the "NMC Early Run," which provides guidance over North America as quickly as possible (Black et al. 1993); subsequent use of the term "early" in this note will be in conjunction with forecasts produced by this version of the model. The focus is now turning toward a mesoscale version in order to determine those modifications needed in the present analysis and forecast system to predict various meteorological features and processes pertinent to subsynoptic scales. The anticipated implementation date for the operational version of the mesoscale Eta Model is the summer of 1994.

The primary purpose of this note is to provide a general nontechnical description of the structure, dynamics schemes, and physical parameterizations used in the mesoscale version of the Eta Model; this will include summaries and updates of information in earlier works that covered the model's characteristics (Black 1988; Mesinger et al. 1988; Janjić 1990, 1994) as well as new details. The description of the present state of the model reviews the work of many scientists associated with the Development Division at NMC. After the general overview, precipitation statistics for November 1993 will be presented followed by two brief examples that compare the abilities of the synoptic and mesoscale versions of the model to predict specific mesoscale features and events.

Corresponding author address: Dr. Thomas L. Black, Development Division, National Meteorological Center, W/NMC 22, Room 204, Washington, DC 20233.

2. Model description

a. Structure

1) THE ETA COORDINATE AND THE VERTICAL GRID

The eta vertical coordinate was defined by Mesinger (1984) in order to remove to a large extent the errors that are known to occur when computing the pressure gradient force, as well as the advection and horizontal diffusion, along a steeply sloped coordinate surface. Like the sigma coordinate (Phillips 1957), eta is pressure based and normalized, which means that both share the mathematical advantages of casting the governing equations of the atmosphere into a relatively simple form. The eta coordinate is defined by the relation

$$\eta = \underbrace{\left(\frac{p - p_T}{p_{\rm sfc} - p_T}\right)}_{\sigma}\left[\frac{p_{\rm ref}(z_{\rm sfc}) - p_T}{p_{\rm ref}(0) - p_T}\right], \qquad (1)$$

where p_T is the pressure at the top of the domain (currently 50 hPa in the Eta Model, but this value will be

reduced to about 25 hPa), p_{sfc} and z_{sfc} are the pressure and the elevation of the model's lower boundary, respectively, and p_{ref} is a reference pressure state that is a function of distance above sea level (the standard atmosphere is used). The first factor on the rhs of Eq. (1) is the standard definition of the sigma coordinate. The second factor is a function only of x and y that converts sigma into eta. Additional discussion of the nature of the eta coordinate appears in the appendix.

The mesoscale version that is being run twice per day in an experimental mode uses the same 38 layers as the operational synoptic-scale version because of size limitations dictated by NMC's present computer facilities; however, approximately 50 layers will be used when the mesoscale version itself becomes operational. Although the final placement of these layers is still being determined, one possible configuration is shown in Fig. 1, which depicts the relative thickness of each layer to the nearest hectopascal. The lowest layer is defined to be exactly 20 m deep for the standard atmosphere. The layers above gradually thicken into the midtroposphere where they begin to thin again (with respect to mass). A secondary maximum in resolution appears near the tropopause. Most prognostic variables are carried at the middle of each layer.

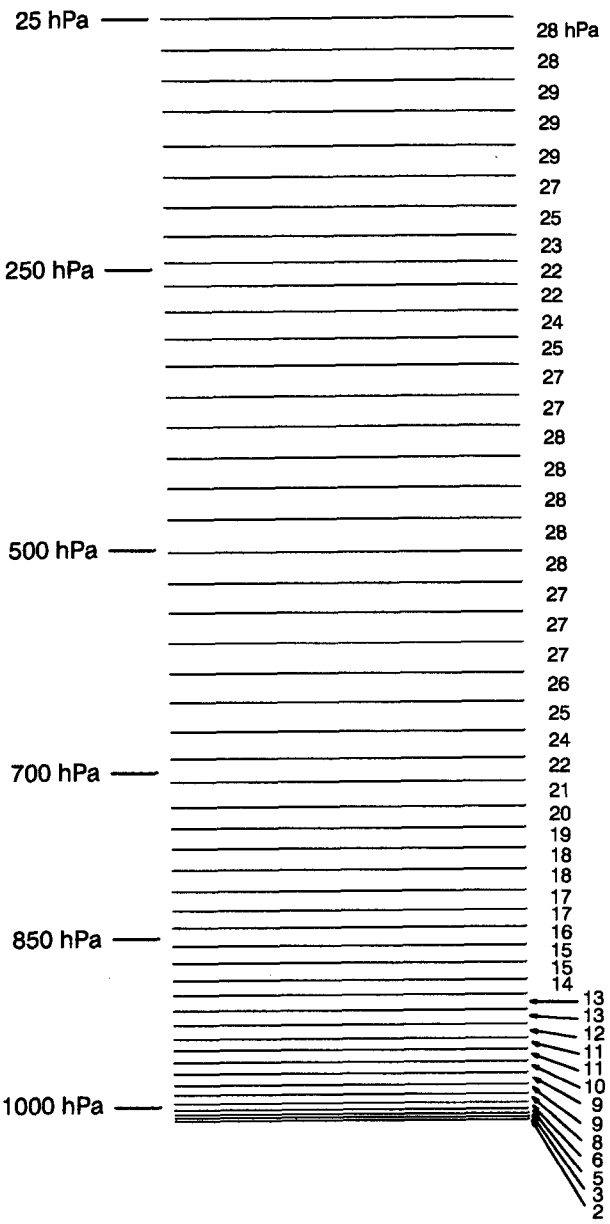

FIG. 1. A sample distribution of the 50 layers in the mesoscale Eta Model. The pressures on the left side indicate the layers' positions with respect to the standard atmosphere, while the numbers on the right give the approximate pressure depth of each layer in hectopascals.

2) THE HORIZONTAL DOMAIN

The semistaggered Arakawa E grid (Winninghoff 1968; Arakawa and Lamb 1977) is the basis of the model's horizontal structure. A sample subset of the E grid is shown in Fig. 2. Each H represents a "mass" variable point (such as temperature or moisture) and each V represents both horizontal components of the wind. The distance "d" is the spacing between adjacent H or adjacent V points, and the magnitude of this distance is commonly used to indicate the model's horizontal resolution. This grid was chosen over the C grid for several reasons. In simulating the geostrophic adjustment process, the C grid displays significant errors for higher internal modes at all wavelengths. While the E grid has an inherent grid separation problem at short wavelengths, a method that greatly reduces this shortcoming has been developed (Mesinger 1973; Janjić 1984). Horizontal advection schemes have been created for both the C and E grids that control the energy cascade to smaller scales (Janjić 1979; Arakawa and Lamb 1981). In the case of the C grid, potential enstrophy is conserved. On the E grid, momentum is conserved and the false energy cascade within the nondivergent part of the flow is constrained to an even greater degree than on the C grid so that any cascade into the two-grid-interval wave is precluded. Last, it appears that the linear amplitude response of forcing by topography in the E grid schemes may be more accurate than that in C grid schemes (Dragosavac and Janjić 1987).

The E grid lies upon a rotated latitude–longitude framework. This coordinate system is created by simply rotating the earth's entire geographic latitude–longitude grid so as to place the intersection of the equator and the prime meridian over the center of the forecast area. In so doing, the convergence of the meridians is minimized over this area. Each grid box thus consists of a mass point surrounded by four velocity points, all of which lie along parallels and meridians of rotated latitude–longitude. While the operational synoptic-scale Eta Model has a horizontal resolution of 80 km, the mesoscale version will use a grid spacing of approxi-

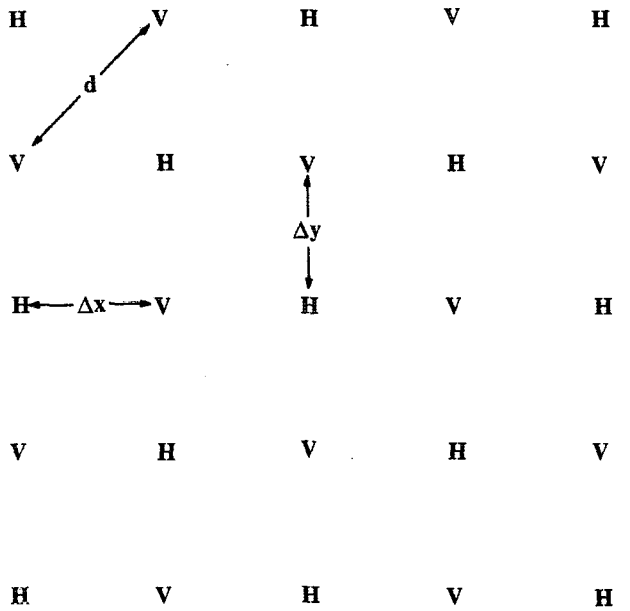

FIG. 2. A subset of the model's Arakawa E grid. Each "H" represents a mass variable, while each "V" represents both horizontal wind components. The values Δx and Δy are the grid increments in the model's rotated latitude–longitude space, while the distance "d" indicates the resolution.

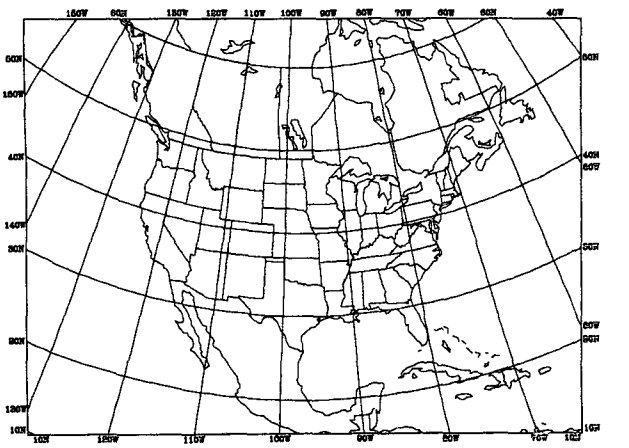

FIG. 3. The approximate horizontal domain of the mesoscale Eta Model.

mately 30 km. The full extent of the mesoscale model's grid will be roughly that shown in Fig. 3.

3) THE STEP-MOUNTAIN TOPOGRAPHY

The model topography is represented as discrete steps whose tops coincide exactly with model layer interfaces (see Mesinger and Collins 1987). In determining their elevations, each horizontal grid box is first divided into 16 subboxes. Actual surface elevations are read from archived data and the mean is taken of all input data points within each subbox. The maximum of these mean values is found from the four subboxes within each of the four rows and four columns of subboxes that lie within each full grid box. The mean of these eight maximum values is then taken to yield an intermediate value for the step height. Having already determined the height of each model layer interface based on the standard atmosphere and the specified distribution of vertical resolution, the final step elevation is found by simply moving each step either upward or downward from its intermediate height to that of the nearest layer interface.

A schematic vertical cross section through the lowest layers of the domain (Fig. 4) illustrates the various aspects of the horizontal and vertical structure. Within each model layer, T represents "mass" variables such as temperature and moisture, while U represents both horizontal components of the wind; p_s is the surface pressure.

All velocity points that lie on the edge of a step are given the value of zero and retain it throughout the forecast (these are indicated by the circled U's in Fig. 4). Because of this no-slip condition, if any grid square lies in a "hole" (it is surrounded by steps of greater elevation in such a way that makes all four surrounding wind points zero) at the end of the process determining step heights described above, the square is raised to the elevation of the lowest interface where at least one of the corner velocity points immediately above that square will not lie along the edge of a higher step, thus allowing the velocity point to be nonzero. This is necessary to ensure that all grid boxes that are above the ground surface are associated with at least one nonzero velocity point; if this were not the case, the horizontal divergence within such a box would always be zero and there could be no communication with the box above through vertical advection.

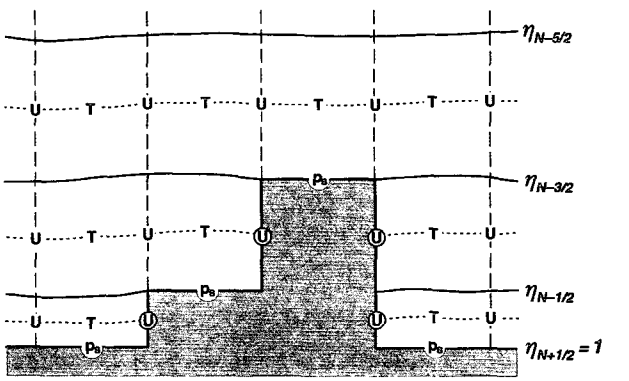

FIG. 4. An idealized vertical cross section of the model's step topography. Each T indicates a "mass" variable within each grid box, while each U represents both horizontal wind components. The quantity p_s is the surface pressure. The circled U's on the sides of steps indicate wind points that are defined as zero at all times.

b. Integration

The primary prognostic variables in the Eta Model are temperature, specific humidity, horizontal wind components, surface pressure, and turbulent kinetic energy. The split-explicit approach is used in producing forecasts based upon these quantities, which means that after each process is computed, each of the relevant variables is updated and the integration proceeds. Because the mesoscale model is designed to support short-range prediction, the forecasts will not exceed 36 h and will be generated twice daily during initial implementation with the goal of eventually generating them four times daily.

1) INITIAL AND BOUNDARY CONDITIONS

While the operational early version uses a purely static data analysis starting from the NMC global forecast first guess, the mesoscale model will receive its initial conditions from the Eta Data Assimilation System (EDAS), now under development, which is analogous to the Regional Data Assimilation System that initializes the Nested Grid Model. The assimilation procedure begins 12 h prior to the actual start of the forecast. At t-12 h, a static analysis is carried out on the model's own grid and coordinate surfaces using a first guess from the Global Data Assimilation System. The model then integrates for 3 h to t-9 h when it stops and new data are assimilated. These steps are repeated until the true start time for the forecast is reached at which point a final analysis is done and the regular forecast begins. By allowing the model to adjust gradually to the analyzed data during the 12-h preforecast period, the typical spinup problems that tend to occur during the early hours of the actual forecast should be significantly reduced. The model's boundary data on its single outermost row of points are obtained by direct interpolation from the aviation run of the global spectral Medium-Range Forecast Model (MRF). At inflow boundary points, all of the prognostic variables are prescribed by the MRF data, while at outflow points, the velocity components tangential to the boundary are extrapolated from the interior of the integration domain. The values in the second outermost row are a blend of those along the boundary and those in the third row that are part of the true integration domain.

2) DYNAMICS

The E grid is essentially a superposition of two C grids. When only the adjustment terms in the equations of motion and continuity are considered, it may be shown that two large-scale solutions from each C grid may exist independently, and a noisy total solution results. In its inertial gravity wave adjustment stage, the Eta Model employs the forward–backward scheme modified in a way that prevents gravity wave separation and thereby precludes the need for explicit filtering (Mesinger 1973; Mesinger and Arakawa 1976; Janjić 1979). The stability criterion allows a doubling of the time step compared to an analogous leapfrog setup, and no computational mode is produced. The fundamental time step is that of inertial gravity wave adjustment. In the 30-km mesoscale version, this will be equal to about 72 s.

The time step for the advection stage is twice that of the adjustment. The horizontal advection scheme was developed by Janjić (1984) specifically for the E grid and controls the cascade of energy toward smaller scales. It is used in conjunction with a modified Euler-backward time-differencing scheme that results in significantly less damping than occurs in the standard Euler-backward scheme for nonmomentum quantities and no damping of the wind components. Because insufficient information is available for the horizontal advection scheme within the five outer rows of the domain, and in order to minimize any impact from possible reflections at the boundaries, an upstream scheme is used for points in the third, fourth, and fifth outermost rows. A simple momentum and energy-conserving centered difference in space with the standard Euler-backward time scheme is used for computing the vertical advection of all quantities except water vapor. With regard to specific humidity, the creation of false maxima and minima in the vertical profile of moisture as vertical advection proceeds is a well-known problem. These artificial extrema may create or exacerbate inaccuracies in the computation of latent heating and precipitation. To circumvent this problem, a piecewise linear method is used that strictly maintains monotonicity in calculating the vertical advection of specific humidity (Van Leer 1977; Mesinger and Janjić 1990).

After each adjustment time step, a second-order nonlinear horizontal diffusion is applied to each of the primary prognostic variables (Janjić 1990) that is similar to that of Smagorinsky (1993) yet differs from it in particular aspects. It should be noted at this point that while the model makes use of horizontal diffusion, it is not needed to maintain numerical stability. The magnitude of this diffusion is derived from the deformation of the wind field and the turbulent kinetic energy. There is no enhancement of diffusion near the lateral boundaries.

3) PHYSICS

Both grid scale and convective precipitation are predicted. After every two adjustment time steps, grid-scale precipitation is formed if the relative humidity in a grid box exceeds 95%. Part or all of this precipitation may evaporate if it falls through layers where the relative humidity is less than 95%. Convective precipitation, based on the Betts–Miller cumulus parameterization (Betts 1986; Betts and Miller 1986) with some of the modifications described by Janjić (1993), is computed every four adjustment time steps. Non-

precipitating shallow convection serves to carry moisture upward and to maintain low-level temperature inversions. Deep convection transports heat and moisture upward and produces rainfall. For both types of convection, reference profiles of temperature and specific humidity are constructed using the values of these variables that are present in the model in conjunction with specified vertical gradients that were determined from numerous observations. The model values are then relaxed toward the reference values. The rainfall is deduced from the net negative change of specific humidity in the deep convective cloud; if the net change in water vapor is positive (net evaporation rather than condensation occurred), no adjustment of the variables is made at that grid point. An explicit cloud water parameterization (Zhao et al. 1991) is now being tested and current plans call for its inclusion in the mesoscale model when it becomes operational.

The calculation of vertical turbulent exchange largely follows that described by Mellor and Yamada (1974, 1982) and is carried out every four adjustment time steps. Exchange between model layers in the free atmosphere is based on the Mellor–Yamada Level 2.5 Model. In this scheme, turbulent kinetic energy (TKE) is a fully prognostic variable that is carried on layer interfaces in the Eta Model. The solution of the production–dissipation part of the predictive equation for TKE is obtained from analytic integration through the time step while also considering physical realizability constraints (Gerrity et al. 1994); changes in TKE due to vertical diffusion and advection are found numerically. Once the TKE is updated, it is used to compute exchange coefficients for the transfer of heat, moisture, and momentum between adjacent model layers. Exchange between the earth's surface and the lowest model layer uses the Mellor–Yamada Level 2 Model in which TKE is assumed to be constant. Surface fluxes are determined using Monin–Obukov functions obtained by numerical integration of appropriate expressions resulting from the Mellor–Yamada Level 2 Model (Łobocki 1993). Compared to an earlier scheme that relied on a finite-difference calculation of the gradient Richardson number, this method may reduce the effect of poorer vertical resolution in thicker model layers that lie over elevated terrain. A viscous sublayer is present over water surfaces in order to describe the difference in values of temperature, moisture, and momentum at the surface itself and what the bulk atmosphere feels. This sublayer has been parameterized as a constant-gradient simplification of the relations of Liu et al. (1979) with various parameters prescribed according to experimental results from Mangarella et al. (1973).

There is currently only one prognostic ground layer but multiple layers will be introduced in the future. The temperature and moisture at the ground surface are updated every four adjustment time steps; over open water these quantities are held constant. The surface soil temperature is computed using a force–restore relation. A Penman–Monteith type of scheme for ground evaporation (Pan 1990) is being tested and will probably be incorporated.

The model's radiation package is virtually identical to that of the MRF and was developed at the Geophysical Fluid Dynamics Laboratory. The shortwave

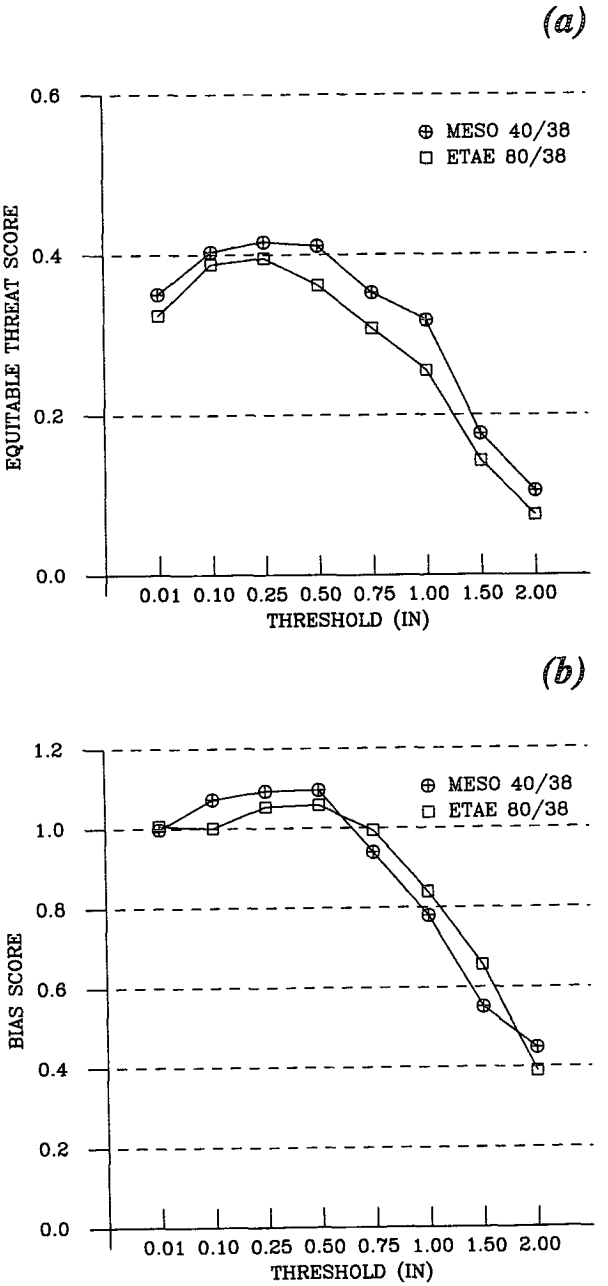

FIG. 5. Skill scores from the combined 0–24-h and 12–36-h precipitation forecasts of the early Eta (ETAE) and the daily test version of the mesoscale model (MESO) for November 1993. The numbers along the abscissas are the precipitation thresholds (in.): (a) the equitable threat scores, and (b) the bias scores.

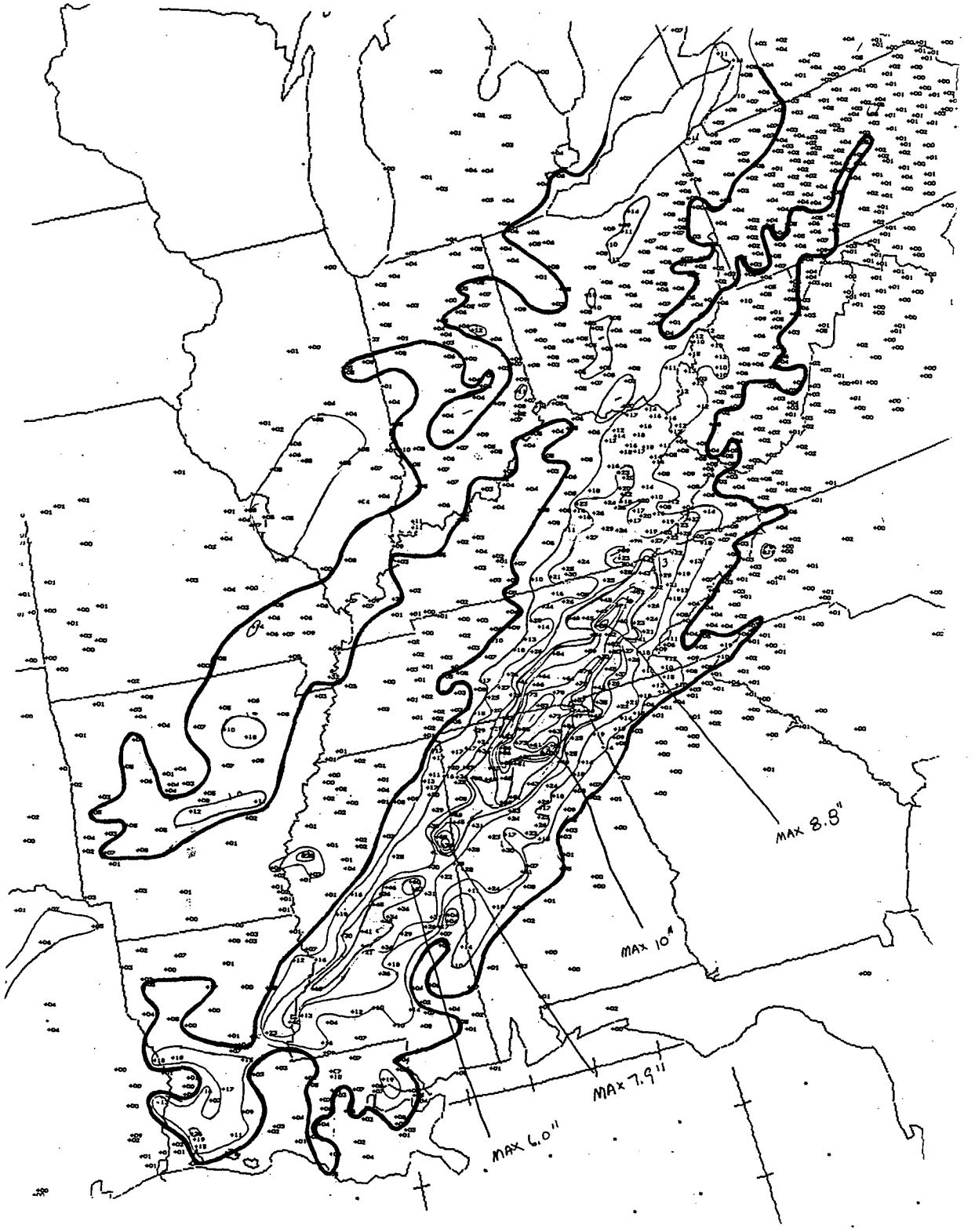

FIG. 6. NMC hand analysis of the 24-h accumulated precipitation (0.1 in.) for the period ending at 1200 UTC 23 December 1990. The 0.5-in. contour has been highlighted. The contour interval is 1 in. for all amounts greater than 0.5 in.

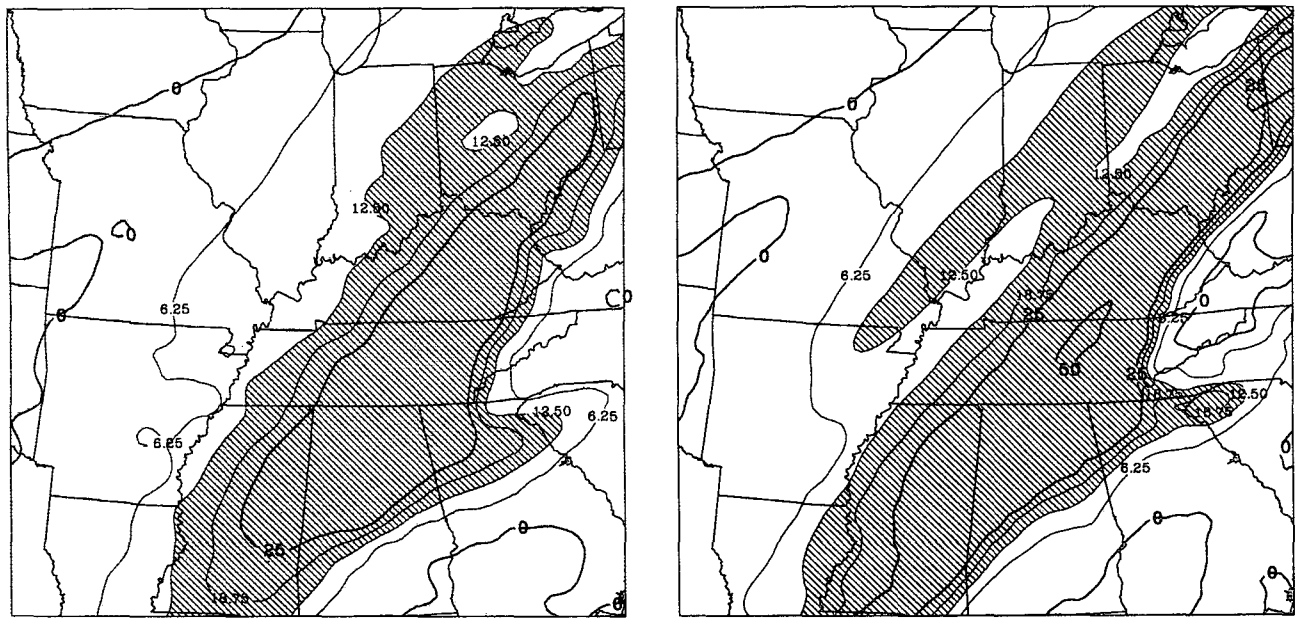

FIG. 7. The 24-h forecasts of 24-h accumulated precipitation of the early (left) and mesoscale (right) versions of the Eta Model valid at 1200 UTC 23 December 1990. The contour interval is 6.25 mm for amounts less than 25 mm, and it is 25 mm for amounts that exceed 25 mm. Hatching covers areas with a total greater than 12.5 mm.

radiation computation scheme is that of Lacis and Hansen (1974), and the longwave scheme is that of Fels and Schwarztkopf (1975). Both are currently executed every two forecast hours although the shortwave calculation will be changed to hourly in order to better resolve the sun's position. Carbon dioxide and ozone distributions are taken from climatology, as is the initial surface albedo, although the latter is allowed to evolve

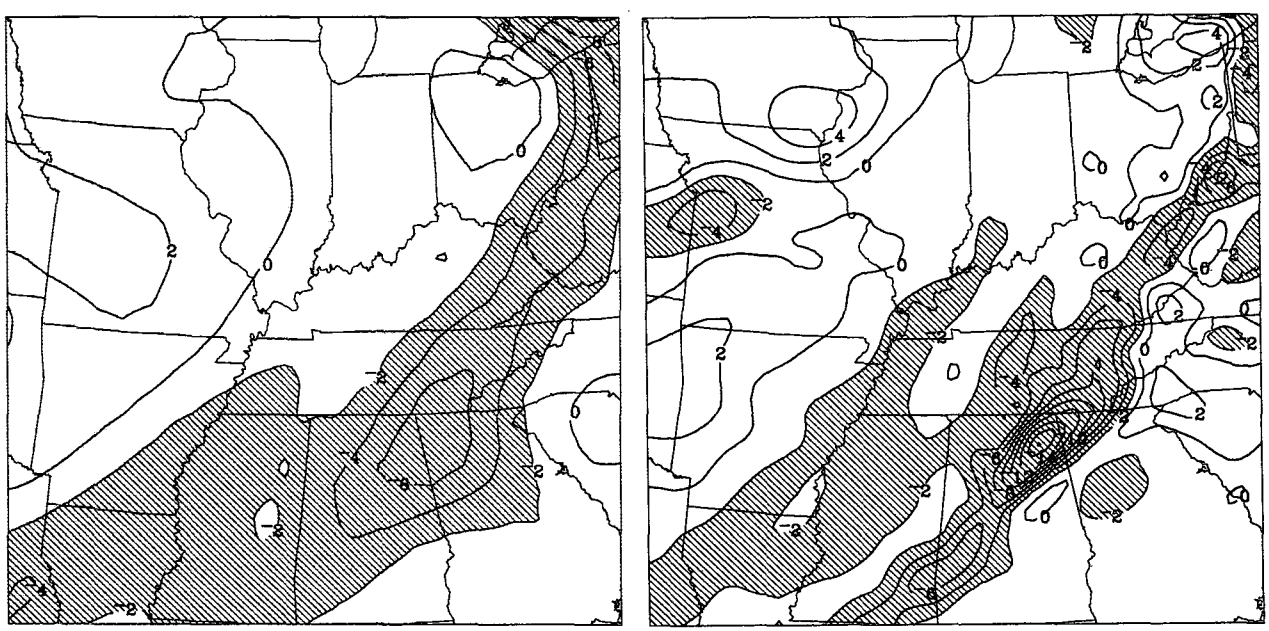

FIG. 8. The 24-h forecasts of 600-hPa vertical velocity (10^{-3} hPa s^{-1}) from the early (left) and mesoscale (right) versions of the Eta Model valid at 1200 UTC 23 December 1990. The contour interval is 2 10^{-3} hPa s^{-1}. Hatching covers areas where the values are less than -2 10^{-3} hPa s^{-1}.

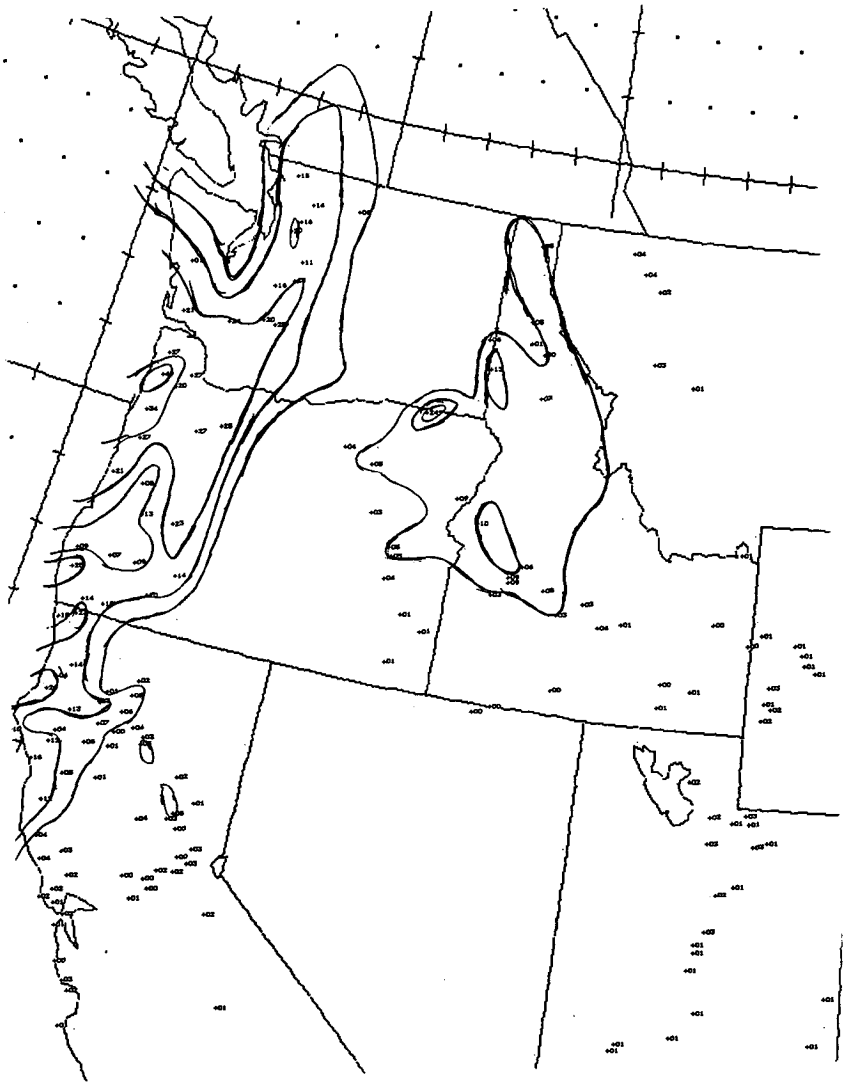

FIG. 9. NMC hand analysis of the 24-h accumulated precipitation (0.1 in.) for the period ending 1200 UTC 22 November 1992. The 0.5-in. contour is drawn, and then the contour interval is 1 in. for all greater amounts.

during the forecast. Both stratiform and cumuliform interactive clouds are diagnosed (generally following Slingo 1987) based upon the model's relative humidity and convective rainfall rate. The atmospheric temperature tendencies arising from the radiative effects are applied after every adjustment time step.

c. Postprocessing

While a standard output package exists for the synoptic-scale version of the model (Treadon 1993), the package for the mesoscale version is still under development. It is envisioned that output will be available at every 25–50 hPa on the model's grid every 3 h. In addition to full fields on the grid, individual station soundings will be generated for each forecast hour. Due to the large volume of output, the forecast data will be available on the Automation of Field Observations and Service data distribution system in gridded form only. Other sources of the model's output will reside at NMC and be accessible via remote retrieval.

3. Precipitation statistics for November 1993

Monthly precipitation statistics from the mesoscale model have been generated from its forecasts since February 1992 when a high-resolution model began running daily. Typically, these data have indicated greater skill at most precipitation thresholds in the mesoscale forecasts than in those of the early Eta by varying amounts. The primary statistics considered are the equitable threat score (ETS) and the bias. Whereas the

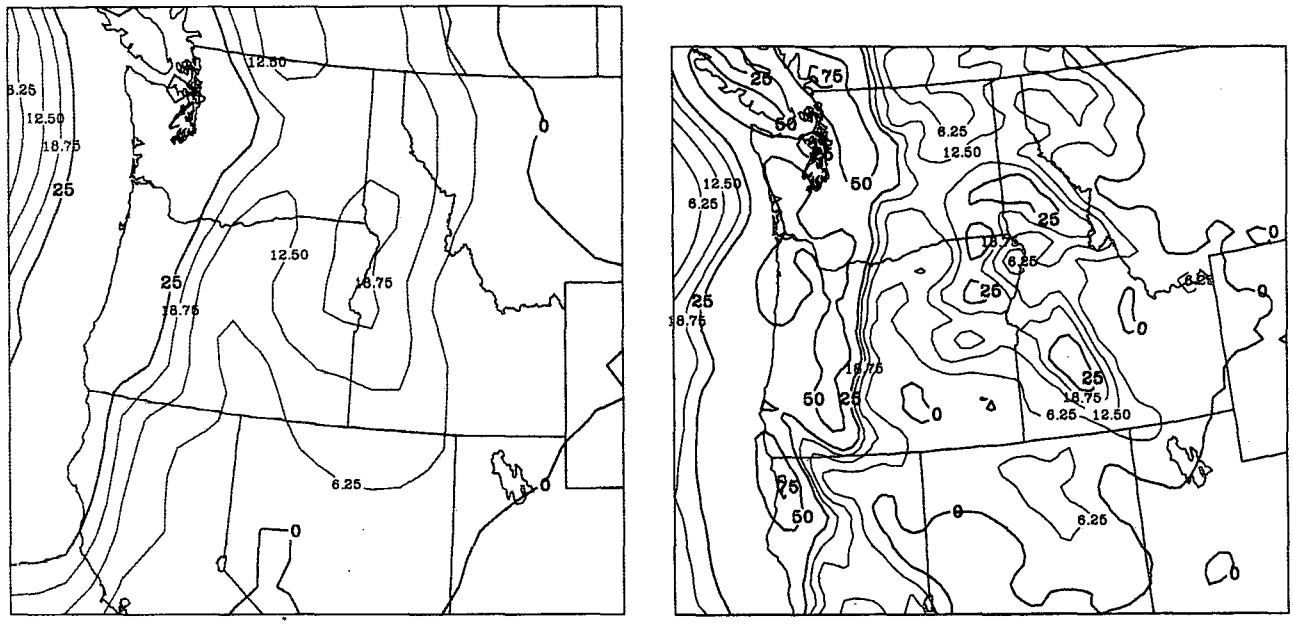

FIG. 10. The 36-h forecasts of 24-h accumulated precipitation from the early (left) and mesoscale (right) versions of the Eta Model valid at 1200 UTC 22 November 1992. The contour interval is 6.25 mm for amounts less than 25 mm, and it is 25 mm for amounts greater than 25 mm.

simple threat score is the quotient of the intersection of the observed and forecast areas of precipitation ("hits") divided by the union of these areas, the ETS refines the definition by accounting for apparent skill derived only from random chance. This is done by replacing the hits in the original formulation with the number of hits above the expected number when forecasting at random (Schaefer 1990). An ETS equal to unity would indicate a perfect forecast; it cannot exceed unity. The bias score does not quantify the accuracy of precipitation forecasts with respect to location as the ETS does but instead simply states the ratio of the total amount of precipitation produced by the model to that which was observed. Again, a score of unity is perfect but it can be either less than one (forecasts are too dry) or greater than one (forecasts are too wet).

The most recent scores available at the time of this writing were for November 1993. Figure 5a shows the ETS from the test version of the mesoscale model that has run twice daily (40-km resolution with 38 layers) and from the early Eta for that month. The truth consists of all 24-h precipitation amounts ending at 1200 UTC obtained from the River Forecast Center data. Both the 0–24-h and the 12–36-h forecasts that end at 1200 UTC are included. For consistency, the analyses are done on the early Eta 80-km grid, and the mesoscale forecasts are interpolated to that grid (in a manner that conserves total water). The graph shows the higher skill in the mesoscale model's forecasts over those of the early Eta at all precipitation thresholds up to 2 in. The bias scores in Fig. 5b show that the total water produced was rather similar for both versions with the mesoscale model being slightly wetter than the early Eta at lighter amounts and drier at heavier amounts. Each generated roughly the proper amount of precipitation for values less than or equal to 0.75 in. As the thresholds increase, the amount of precipitation in the forecasts becomes continually smaller with respect to what was observed.

4. Forecast examples

Specific aspects of two different forecasts will now be discussed very briefly in order to preview the types of improvements that can be realized in the mesoscale model's predictions. The first involves what is primarily a purely dynamical situation, while the second describes the interaction of synoptic-scale dynamics with orography. Since the EDAS is not complete at the time of this writing, the mesoscale model's forecasts were initialized by simply interpolating the 0-h forecast from the Nested Grid Model into the former's domain. The early version was initialized in precisely the same manner as the mesoscale model in these two examples, so that there would be no differences in initial conditions. The boundary conditions were also produced in the same way for each version by using the aviation forecast commencing at the same time that the sample Eta forecasts began.

a. Frontal-related circulation in the central United States

On 22 and 23 December 1990, a strong Arctic cold front moved southeastward across the Mississippi and

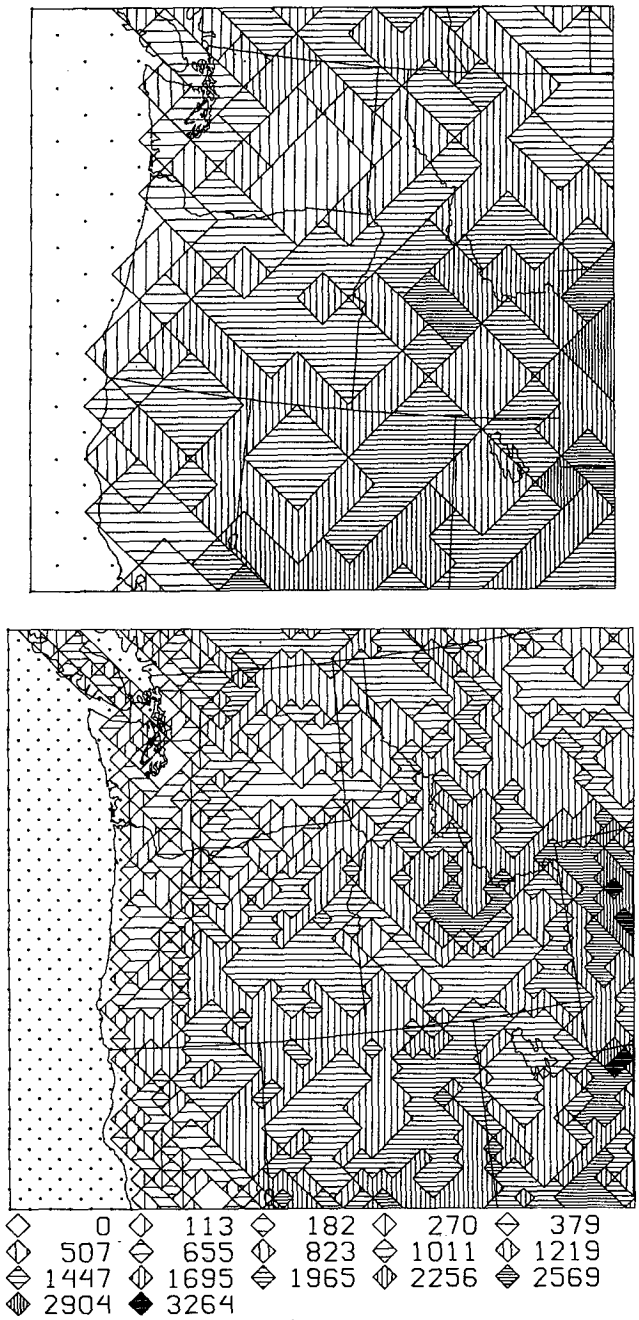

FIG. 11. The surface elevation (m) in the early (above) and mesoscale (below) versions of the Eta Model. The key at the bottom is valid for both diagrams. The dots are mass point locations over water on the model grids.

Ohio Valleys bringing temperatures that ranged from around 20°F immediately behind the front to subzero farther to the northwest. Ahead of the front in Alabama, Mississippi, and Tennessee was a region of warm, unstable air with temperatures up to around 60°F and dewpoints in the upper 50's. Thunderstorms in advance of the front were responsible for a major precipitation event. Figure 6 shows the NMC hand analysis of the 24-h accumulated precipitation for the period ending 1200 UTC 23 December 1990. Amounts exceeding 3 in. (75 mm) covered a sizable area from northern Mississippi into Tennessee. In addition to this heavy convective rainfall, a distinct narrow band of lighter precipitation occurred somewhat to the northwest in a line from Arkansas northeastward into Indiana as seen by the highlighted 0.5-in. (12.5 mm) contour.

Forecasts from 1200 UTC 22 December were made from the early Eta Model with 80-km horizontal resolution and 38 layers, as well as from the mesoscale version with 30-km resolution and 50 layers. In both this case and the one that follows, the configuration of the 50 layers is that given in Fig. 1. The 24-h accumulated precipitation predicted through 1200 UTC 23 December (Fig. 7) indicates the advantages of the mesoscale run. Although neither version produced the very heavy rainfall associated with the convection in the warm sector ahead of the front, the mesoscale forecast does show a slightly larger area of 50 mm. Part of the problem may arise from the lack of a preforecast spinup period in either version. A notable difference though is seen in the fact that there is almost no hint of the narrow band of lighter precipitation in the early forecast, while it is clearly present in that of the mesoscale run with the 12.5-mm contour corresponding well with the 0.5-in. contour in Fig. 6.

As further evidence that the mesoscale forecast did indeed capture a smaller-scale circulation behind the primary one at the leading edge of the front, the instantaneous 600-hPa omega fields at the end of the 24-h forecast period are depicted in Fig. 8. The early forecast produced a relatively broad region of upward motion in the midtroposphere associated with the advancing front and predicted a maximum of 6 10^{-3} hPa s^{-1} over extreme northwest Georgia. A slight hint of a second region of upward motion can be seen in western Tennessee. The mesoscale forecast shows a stronger, more focused strip of upward motion near the front and a maximum of 18 10^{-3} hPa s^{-1} over northeast Alabama. In addition, the second weaker band is apparent from southeast Arkansas to southern Indiana. Clearly in this instance the higher spatial resolution of the mesoscale version of the model resulted in its being able to describe the much weaker secondary circulation that the coarser resolution of the early version precluded.

b. Orographically forced circulations in the Pacific Northwest

In contrast to the previous case, which took place in the relatively flat Midwest and South with only secondary effects caused by the western slopes of the Appalachians, this event occurred in the northwest United States where the interaction of complex terrain with

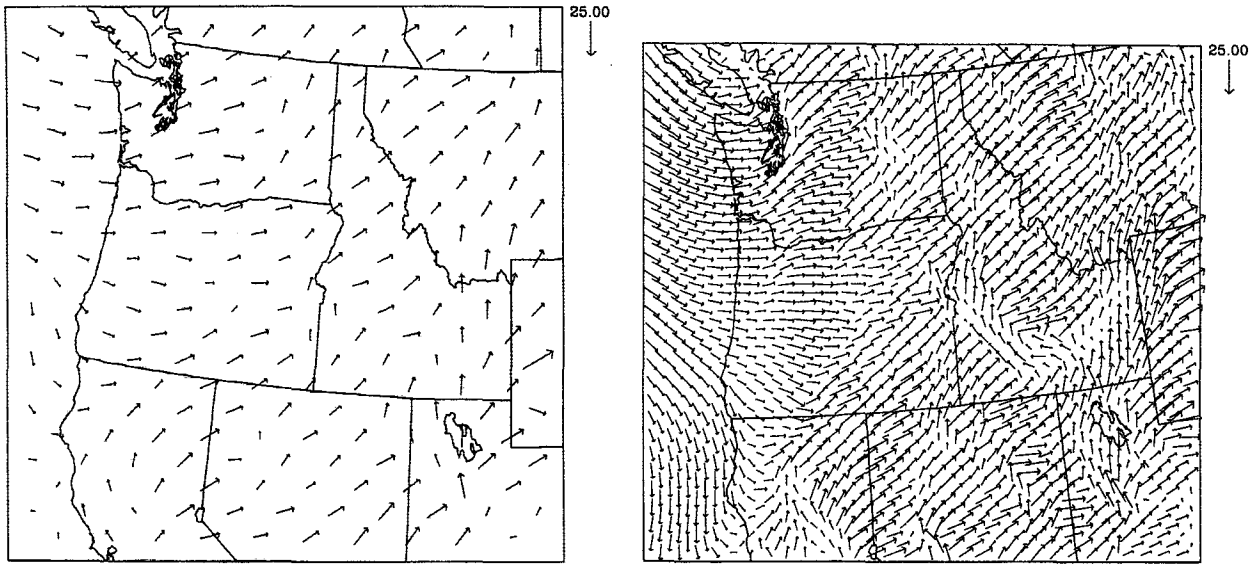

FIG. 12. The 36-h forecasts of lowest layer winds from the early (left) and mesoscale (right) versions of the Eta Model. Each arrow represents the wind vector at the models' velocity grid points. The arrow at the top right of each diagram indicates the length of a 25 m s^{-1} wind vector.

the synoptic-scale flow was paramount in determining the nature of the lower-level circulations. On 20 November 1992, a low pressure center was positioned well out to sea, west of Vancouver Island. By 22 November, it had moved onshore and into southern British Columbia, trailing a cold front to the southwest across Washington, Oregon, and extreme northern California. Both the early and the mesoscale versions of the Eta Model were run from initial conditions at 0000 UTC 21 November 1992.

A signature of the circulations forced by the region's mountainous topography is seen in NMC's hand analysis of the 24-h accumulated precipitation for the period ending 1200 UTC 22 November 1992 (Fig. 9). Amounts exceeding 2 in. (50 mm) fell all along the windward side of the Cascades in Washington and Oregon. A local maximum of 4 in. (100 mm) occurred near the northwest Oregon coast. Several local 2 in. (50 mm) maxima were located in southwest Oregon and northwest California. Farther inland, other separate maxima are seen in western Idaho and near the eastern end of the Washington–Oregon border.

The corresponding forecasts from the two versions of the model (Fig. 10) indicate considerable differences in the details of the rainfall patterns. The early run shows a fairly smooth area along the coast with totals in excess of 25 mm all the way from Canada to California. One inland maximum was present as a single center of less than 25 mm where Idaho, Washington, and Oregon meet. In contrast, the mesoscale run predicted (a) a 50-mm strip on the windward side of the Cascades, (b) a local maximum of nearly 75 mm on the northwest Oregon coast, (c) another maximum of 50–75 mm in southwest Oregon and northwest California, and (d) individual 25-mm maxima in western Idaho and on the eastern end of the Washington–Oregon border. Each of these details seems to agree rather well with the observations in Fig. 9.

Of course, these improvements in the mesoscale forecast arise primarily from its higher-resolution representation of the area's landforms, which is apparent in Fig. 11, where the two versions' step topographies are depicted. While the 80-km steps do indicate some of the grosser details of the Cascades and Rockies, they are naturally unable to describe the details seen in the 30-km steps where many more of the local variations present in the actual surface elevation have been approximated. Another manifestation of the greater accuracy in representing these surface features appears in the forecasts of the lowest-layer winds at 1200 UTC 22 November (Fig. 12). The velocity vectors are drawn at each velocity point on each of the models' semi-staggered grids. Considerably more detail in the deviation of these winds by the orography is immediately seen in the mesoscale model's prediction over that of the early run throughout the entire area shown.

5. Summary

After replacement of the LFM with the early synoptic-scale version of the Eta Model in June 1993, a new mesoscale version is planned for implementation in the summer of 1994. Its purpose will be to augment the current array of operational synoptic-scale numer-

ical forecasts with guidance down to mesoscale ranges at least twice daily out to 24–36 h over the 48 contiguous states. Preliminary results indicate that the mesoscale version of the model is capable of capturing at least some small-scale circulations, forced by either internal dynamics alone or by orography, with reasonable accuracy. This is the first time NMC will generate operational mesoscale forecasts. It will be a challenging task because mesoscale prediction raises some very complex issues, particularly when constrained by an operational environment. Collaboration with field forecasters will be an important part of NMC's efforts in continuing to improve the numerical guidance.

Acknowledgments. The author hastens to acknowledge all of the individuals inside and outside of the Development Division who have made invaluable contributions to the development of the Eta Model. The author is very grateful to Dr. Fedor Mesinger for his useful comments offered during the preparation of this note. Suggestions from Drs. Eugenia Kalnay, Geoff DiMego, Louis Uccellini, and Brad Colman were also very helpful. I want to thank Dr. Ron McPherson and Dr. Kalnay for their continued support of this effort in mesoscale numerical weather prediction. The value of the feedback received from forecasters during the past and future development of the Eta Model cannot be overstated.

APPENDIX

A General Description of the Eta and Sigma Coordinates

The following discussion illustrates the advantages of the simple relationship given in Eq. (1) that defines eta. Both sigma and eta identify the vertical position of a point in the atmosphere as the ratio of the pressure difference between the point in question and the top of the domain (TOD) to that of the pressure difference between a fundamental base below the point and TOD. Thus, sigma and eta each vary from zero at TOD to unity at the base. In the case of sigma, the fundamental base is at the model's ground surface. Figure A1a shows two points, P1 and P2, that are exactly the same elevation above mean sea level (MSL), but P1 lies on the ground at the top of a mountain while P2 is in the free atmosphere. This means that the sigma value at P1 is equal to one; at P2, sigma is significantly less than one because the pressure difference between P2 and TOD is considerably less than that between the ground directly beneath P2 and TOD. In other words, although the pressure difference between P1 and TOD is similar to that between P2 and TOD, the sigma values at those locations differ markedly because the values of *surface pressure* at the ground below those points minus TOD are very different. The end result is that the sigma coordinate surfaces follow the model terrain and are steeply sloped in regions where the topography itself is steeply sloped.

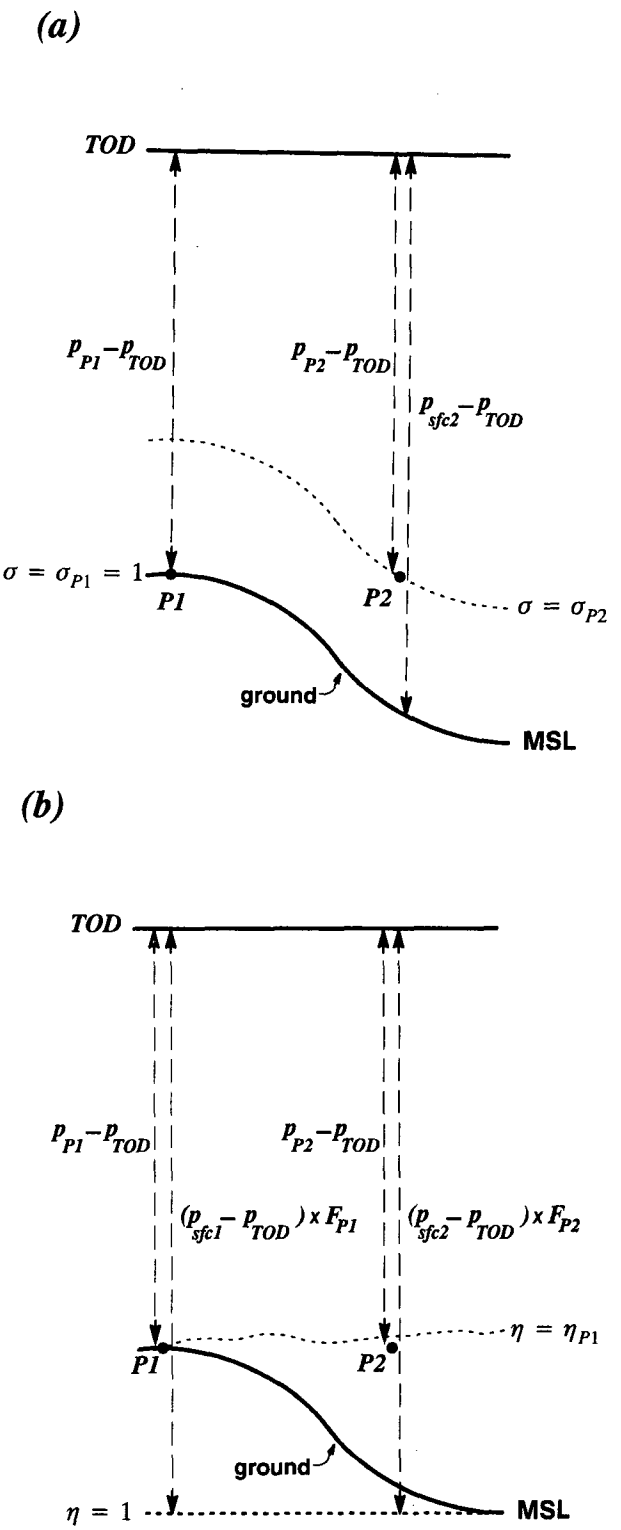

FIG. A1. A point P1 located at the ground on a mountaintop and a point P2 adjacent to P1 at the same height above mean sea level (MSL) but in the free atmosphere. (a) In a sigma coordinate framework, a coordinate surface (thin dashed line) must slope steeply following the terrain. (b) In an eta coordinate framework, a coordinate surface is relatively horizontal regardless of the terrain.

The fundamental base in eta coordinates is not at the ground surface but is instead at MSL. To compute the pressure difference between the base and TOD, the pressure difference between the ground surface and TOD is increased using a factor F derived from the height–pressure relationship of the standard atmosphere so as to yield the pressure difference between MSL and TOD; this extrapolation factor is the bracketed quantity in the denominator of Eq. (A1), which is simply a rewriting of Eq. (1):

$$\eta = \frac{p - p_T}{(p_{\text{sfc}} - p_T)\underbrace{\left[\frac{p_{\text{ref}}(0) - p_T}{p_{\text{ref}}(z_{\text{sfc}}) - p_T}\right]}_{F}}. \qquad \text{(A1)}$$

Figure A1b shows the same situation as Fig. A1a except in terms of the eta coordinate. The long vertical arrows represent the denominator of Eq. (A1) where the ground-to-TOD pressure difference has been increased to that of MSL-to-TOD by the extrapolation factor F computed at each horizontal location. The eta values at each point can now be determined by taking the ratio given in Eq. (A1). A line of constant eta value equal to that at P1 is seen to pass very near P2. This means that because the pressure difference between P1 and TOD is very similar to that between P2 and TOD in addition to the fact that the values of *mean sea level pressure* below these points minus TOD are also very similar, then the values of eta at P1 and P2 are also similar. The result of the relation given in Eq. (1) and Eq. (A1) is thus a coordinate whose surfaces remain relatively horizontal at all times while retaining the mathematical advantages of a pressure-based system that does not intersect the ground as stated earlier.

REFERENCES

Arakawa, A., and V. R. Lamb, 1977: Computational design of the basic dynamical processes of the UCLA general circulation model. *Methods Comput. Phys.*, **17**, 173–265.

—— and ——, 1981: A potential enstrophy and energy conserving scheme for the shallow water equations. *Mon. Wea. Rev.*, **109**, 18–36.

Betts, A. K., 1986: A new convective adjustment scheme. Part I: Observational and theoretical basis. *Quart. J. Roy. Meteor. Soc.*, **112**, 1306–1335.

——, and M. J. Miller, 1986: A new convective adjustment scheme. Part II: Single column tests using GATE wave, BOMEX, and arctic air-mass data sets. *Quart. J. Roy. Meteor. Soc.*, **112**, 693–709.

Black, T. L., 1988: The step-mountain eta coordinate regional model: A documentation. NOAA/NWS/, 47 pp. [Available from the National Meteorological Center, NOAA Science Center, Room 204, 5200 Auth Road, Camp Springs, MD 20746.]

——, D. G. Deaven, and G. DiMego, 1993: The step-mountain eta coordinate model: 80 km 'Early' version and objective verifications. Technical Procedures Bulletin 412, NOAA/NWS, 31 pp. [Available from the National Weather Service, Office of Meteorology, 1325 East-West Highway, Silver Spring, MD 20910.]

Dragosavac, M., and Z. I. Janjić, 1987: Topographically induced stationary solutions of linearized shallow water equations on various grids. *Mon. Wea. Rev.*, **115**, 730–736.

Fels, S. B., and M. D. Schwarztkopf, 1975: The simplified exchange approximation: A new method for radiative transfer calculations. *J. Atmos. Sci.*, **32**, 1475–1488.

Gerrity, J. P., T. L. Black, and R. E. Treadon, 1994: On the numerical solution of the Mellor–Yamada level 2.5 turbulent kinetic energy equation in the Eta Model. *Mon. Wea. Rev.*, **122**, in press.

Janjić, Z. I., 1979: Forward-backward scheme modified to prevent two-grid-interval noise and its application in sigma coordinate models. *Contrib. Atmos. Phys.*, **52**, 69–84.

——, 1984: Nonlinear advection schemes and energy cascade on semi-staggered grids. *Mon. Wea. Rev.*, **112**, 1234–1245.

——, 1990: The step-mountain coordinate: Physical package. *Mon. Wea. Rev.*, **118**, 1429–1443.

——, 1994: The step-mountain eta coordinate model: Further developments of the convection, viscous sublayer, and turbulence closure schemes. *Mon. Wea. Rev.*, **122**, 927–945.

Lacis, A. A., and J. E. Hansen, 1974: A parameterization of the absorption of solar radiation in the earth's atmosphere. *J. Atmos. Sci.*, **31**, 118–133.

Liu, W. T., K. B. Katsaros, and J. B. Businger, 1979: Bulk parameterization of air–sea exchanges of heat and water vapor including the molecular constraints at the interface. *J. Atmos. Sci.*, **36**, 1722–1735.

Łobocki, L., 1993: A procedure for the derivation of surface-layer bulk relationships from simplified second-order closure models. *J. Appl. Meteor.*, **32**, 126–138.

Mangarella, P. A., A. J. Chambers, R. L. Street, and E. Y. Hsu, 1973: Laboratory studies of evaporation and energy transfer through a wavy air-water interface. *J. Phys. Oceanogr.*, **3**, 93–101.

Mellor, G. L., and T. Yamada, 1974: A hierarchy of turbulence closure models for planetary boundary layers. *J. Atmos. Sci.*, **31**, 1791–1806.

——, and ——, 1982: Development of a turbulence closure model for geophysical fluid problems. *Rev. Geophys. Space Phys.*, **20**, 851–875.

Mesinger, F., 1973: A method for construction of second-order accuracy difference schemes permitting no false two-grid-interval wave in the height field. *Tellus*, **25**, 444–458.

——, 1984: A blocking technique for representation of mountains in atmospheric models. *Riv. Meteor. Aeronaut.*, **44**, 195–202.

——, and A. Arakawa, 1976: Numerical methods used in atmospheric models. GARP Publ. Series, No. 17, Vol. 1, WMO, Geneva, 64 pp. [Available from WMO/ICSU, Case Postale No. 2300, CH-1121 Geneva 20, Switzerland.]

——, and Z. I. Janjić, 1990: Numerical methods for the primitive equations. *Ten Years of Medium-Range Weather Forecasting*, Reading, United Kingdom, ECMWF, 205–251.

——, ——, S. Ničković, D. Gavrilov, and D. G. Deaven, 1988: The step-mountain coordinate: Model description and performance for cases of Alpine lee cyclogenesis and for a case of Appalachian redevelopment. *Mon. Wea. Rev.*, **116**, 1493–1518.

Pan, H., 1990: A simple parameterization scheme of evapotranspiration over land for the NMC Medium-Range Forecast Model. *Mon. Wea. Rev.*, **118**, 2500–2512.

Phillips, N. A., 1957: A coordinate system having some special advantages for numerical forecasting. *J. Meteor.*, **14**, 184–185.

Schaefer, J. T., 1990: The critical success index as an indicator of warning skill. *Wea. Forecasting*, **5**, 570–575.

Slingo, J. M., 1987: The development and verification of a cloud prediction scheme for the ECMWF model. *Quart. J. Roy. Meteor. Soc.*, **113**, 899–927.

Smagorinsky, J., 1993: Some historical remarks on the use of nonlinear viscosities. *Large Eddy Simulations of Complex Engineering and Geophysical Flows*, B. Galperin and S. Orszag, Eds., Cambridge University Press, 1–34.

Treadon, R. E., 1993: The NMC Eta Model post processor: A documentation. NMC Office Note 394, NOAA/NWS, 44 pp. [Available from the National Meteorological Center, NOAA Science Center, Room 101, 5200 Auth Road, Camp Springs, MD 20746.]

Van Leer, B., 1977: Towards the ultimate conservative difference scheme: A new approach to numerical convection. *J. Comput. Phys.*, **23**, 276–299.

Winninghoff, F. J., 1968: On the adjustment toward a geostrophic balance in a simple primitive equation model with application to the problems of initialization and objective analysis. Ph.D. thesis, University of California, Los Angeles.

Zhao, Q., F. H. Carr, and G. B. Lesins, 1991: Improvement of precipitation forecasts by including cloud water in NMC's Eta Model. Preprints, *Ninth Conf. on Numerical Weather Prediction*, Denver, CO, Amer. Meteor. Soc., 50–53.